Optical and Photoemissive Properties of Nickel in the Vacuum-Ultraviolet Spectral Region*

R. C. VEHSE† AND E. T. ARAKAWA
Health Physics Division, Oak Ridge National Laboratory, Oak Ridge, Tennessee 37830
(Received 21 October 1968)

Measurements of the optical properties of evaporated films of nickel for the spectral region of 4 to 24 eV and of the photoemissive properties of similarly prepared samples for photon energies of 10.2 to 22.4 eV are reported. The optical data were analyzed using a modified form of the Kramers-Kronig method, structure being found in the dielectric functions characteristic of interband transitions of 4.5 and 14.0 eV. The loss function $-\mathrm{Im}(1/\epsilon+1)$, where ϵ is the dielectric constant, shows structure at 8.0 eV, and the loss function $-\mathrm{Im}(1/\epsilon)$ shows structure at 10 and 20 eV associated with plasma oscillations. The photoelectron energy distribution curves are found to be in reasonable agreement with previously reported data for excitation energies below 11.8 eV, except that the contribution attributed to a peak in the density of electronic states 5 eV below the Fermi level is somewhat smaller for freshly prepared films. This contribution to the photoelectron energy distribution for an incident photon energy of 10.2 eV shows a marked temporal dependence for samples prepared and stored *in situ* at 10^{-8} Torr. Evidence is given from the data at higher excitation energies for photoelectron excitation of volume plasmons and for the possible photoelectron excitation of an interband transition.

I. INTRODUCTION

PHOTOEMISSION studies on various transition and noble metals have revealed possible correlations between certain structure in the optical densities of electronic states and the ferromagnetic properties of these elements.[1] For Ni at room temperature, Blodgett and Spicer[2] have identified structure in the density of states at 5 eV below the Fermi level with the ferromagnetic properties of the pure metal. The optical density of states was determined from a series of energy distribution curves for the emitted photoelectrons at excitation energies of 11.8 eV and less, so the structure at 5 eV below the Fermi level in the density of states was obtained from emitted photoelectrons with kinetic energies equal to or less than 2.3 eV, since the work function of Ni is 4.5 eV.[3] The effect of electron-electron scattering and the energy-dependent electron escape function for the photoemission process result in pronounced structure in the energy distribution curves at low-escape energies, and some difficulty is encountered in the determination of the density of states for this region. Consequently, the need for photoemission studies at excitation energies above the LiF cutoff had become evident.

In the work reported here, the energy distribution of the photoelectrons emitted from evaporated films of high purity Ni was measured for excitation energies of 10.2 to 22.4 eV. Also, the optical properties of similarly prepared samples were determined, and these data were correlated with the photoemission data in a manner described earlier[4] for Pd and Ag to provide insight about the inelastic-scattering properties of low-energy electrons in Ni. Previous measurements[5] of the optical properties of electrolytically etched bulk samples of Ni have been made for photon energies in the vacuum uv below the LiF cutoff, but no optical studies have been made for evaporated Ni films in the region above 11.8 eV since the very early work of Sabine.[6] The experimental techniques used in this work are described in the next section, and the experimental results appear in Sec. III. The analysis and discussion of these results, based on the theoretical analyses of optical properties as reviewed by several authors (e.g., Ehrenreich,[7] Pines,[8] and Stern,[9] and on the model for photoemission developed by Berglund and Spicer[10]), are given in Sec. IV.

II. EXPERIMENTAL TECHNIQUES

The Ni samples used in this work were prepared by vacuum evaporation *in situ* at about 10^{-8} Torr from resistance-heated filaments. Precleaned glass microscope slides were used as the substrate material, and the purity of the Ni wire wound on the filaments was given as 99.9995% by the supplier (Leico Industries, Inc., New York, N. Y.). Film thicknesses on the substrate

* This paper is based upon a dissertation submitted by R. C. Vehse in partial fulfillment of the requirements for the Ph.D. degree in physics at the University of Tennessee, Knoxville. The research was sponsored by the U. S. Atomic Energy Commission under contract with Union Carbide Corp.

† Formerly a U. S. Atomic Energy Commission Special Health Physics Fellow, University of Tennessee, Knoxville. Present address: Bell Telephone Laboratories, Reading, Pa.

[1] W. E. Spicer, Phys. Rev. **154**, 385 (1967).

[2] A. J. Blodgett, Jr., and W. E. Spicer, Phys. Rev. **146**, 390 (1966).

[3] V. S. Fomenko, in *Handbook of Thermionic Properties*, edited by G. V. Samsonov (Plenum Press, Inc., New York, 1966), pp. 1–63.

[4] R. C. Vehse, J. L. Stanford, and E. T. Arakawa, Phys. Rev. Letters **19**, 1041 (1967).

[5] H. Ehrenreich, H. R. Philipp, and D. J. Olechna, Phys. Rev. **131**, 2469 (1963).

[6] G. B. Sabine, Phys. Rev. **55**, 1064 (1939).

[7] H. Ehrenreich, in *Proceedings of the International School of Physics "Enrico Fermi," Course 34*, edited by J. Tauc (Academic Press Inc., New York, 1966), pp. 106–154.

[8] D. Pines, *Elementary Excitations in Solids* (W. A. Benjamin, Inc., New York, 1964), pp. 203–228.

[9] F. Stern, in *Solid State Physics*, edited by F. Seitz and D. Turnbull (Academic Press Inc., New York, 1963), Vol. 15, pp. 300–408.

[10] C. N. Berglund and W. E. Spicer, Phys. Rev. **136**, A1030 (1964); **136**, A1044 (1964).

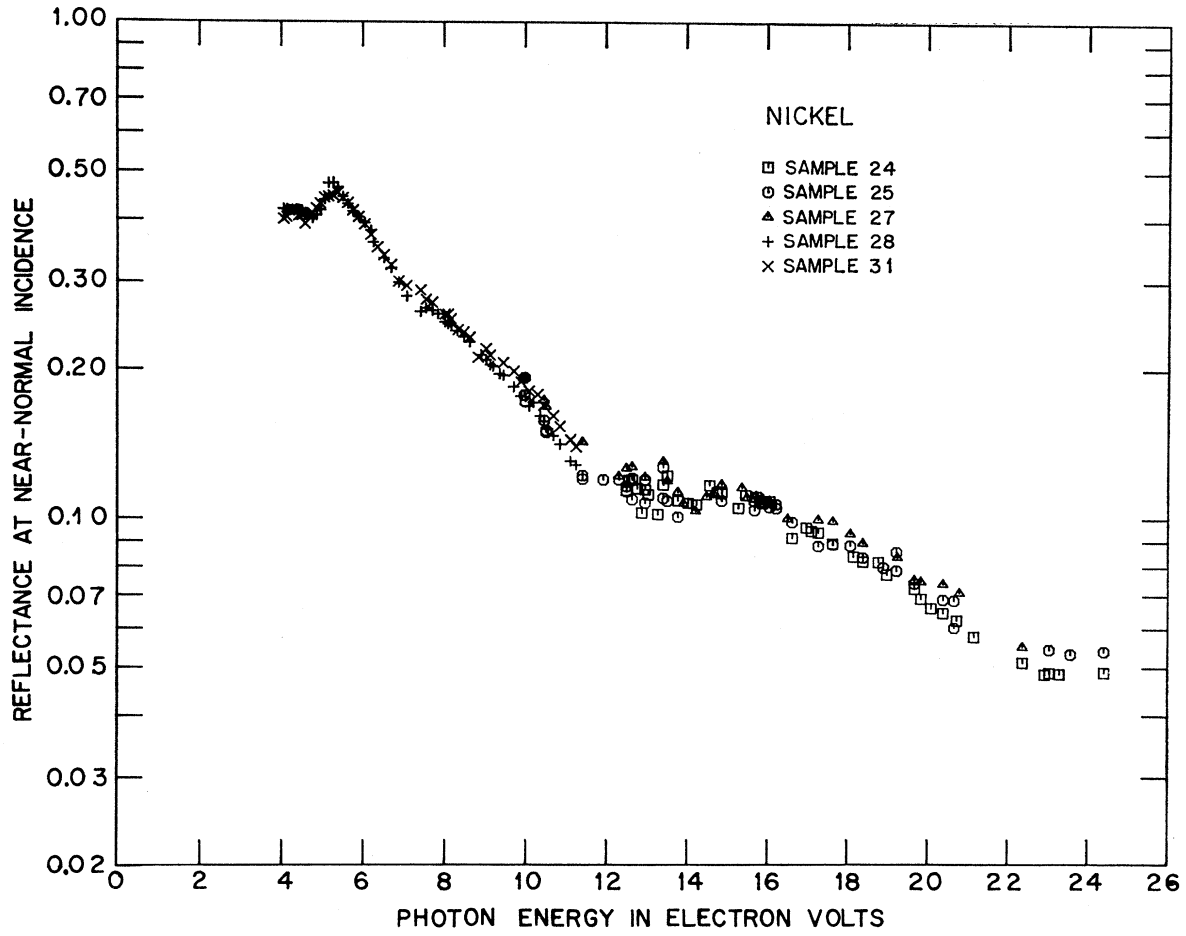

FIG. 1. Near-normal-incidence reflectance data of nickel measured for photon energies of 4–24.5 eV.

ranged from 1800–2200 Å, and the evaporation rate was roughly 150 Å per sec. Measurements were initiated within 1 min following the termination of the evaporation. A complete description of the apparatus used has been given earlier.[11,12]

In order to determine the optical constants, the near-normal reflectance was measured for incident photon energies from 4 to 24 eV together with the reflectances for several angles of incidence at a few selected photon energies. The energy distribution of the emitted photoelectrons was measured by the retarding-voltage technique. A sweep rate was chosen for the retarding potential applied to a cylindrical grid so that the entire photoemission current versus retarding potential curve could be recorded in less than 10 min. The kinetic-energy distribution of photoelectrons for each incident photon energy was obtained by numerical differentiation of the photoemission current versus retarding potential curves. In each case the results were averaged for at least three samples. In the final analysis the area under the energy distribution curve was normalized to the absolute quantum yield at the corresponding photon energy $h\nu$ and the abscissa scale was changed to E^* according to the equation

$$E^* = E + \Phi - h\nu \,, \tag{1}$$

where Φ is the work function of the sample, and E the measured kinetic energy of the emitted photoelectrons.

Time studies indicated that sufficient deterioration of the sample surface occurs within about $\frac{1}{2}$ h after evaporation so that no reliable photoemission data could be obtained for samples over $\frac{1}{2}$ h old. Furthermore, it was found that all reflectance data were not exactly reproducible from sample to sample because of sensitivity in the reflectance of the evaporated film to minor irregularities in the sample surface. Consequently, several samples were prepared and subjected to reflectance measurements for each of the different regions of the spectrum covered by the various light-source gases used. Since generally the highest values of the reflectance in the vacuum uv are obtained by the most exacting conditions of sample preparation, the merits of a "good" sample were judged using this criterion.

[11] R. C. Vehse and E. T. Arakawa, Bull. Am. Phys. Soc. 11, 830 (1966).

[12] R. C. Vehse and E. T. Arakawa, Oak Ridge National Laboratory Report No. ORNL-TM-2240, 1968 (unpublished).

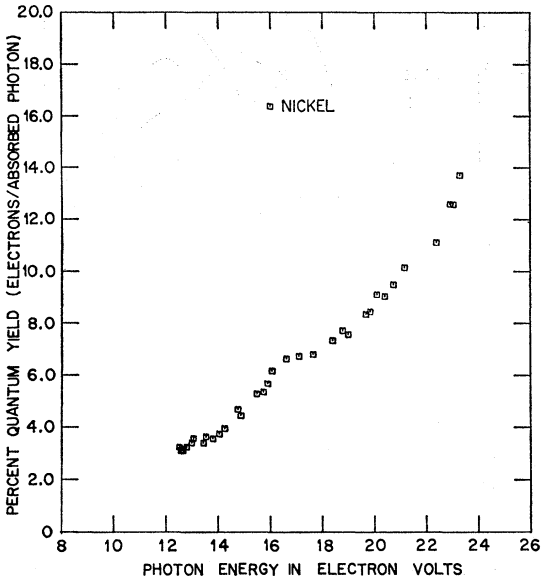

FIG. 2. Spectral distribution of the quantum yield of nickel for excitation energies of 10–24 eV.

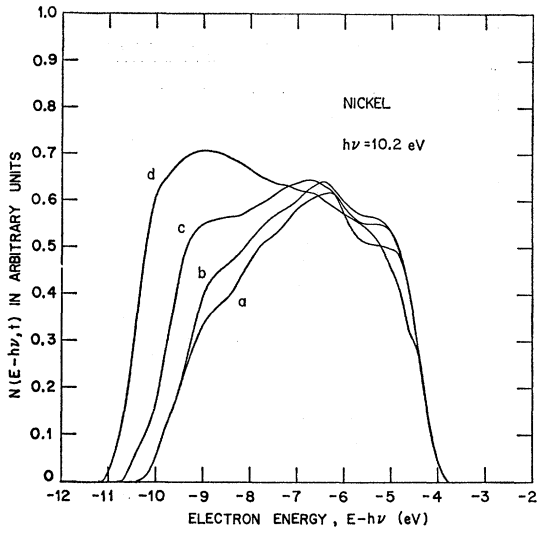

FIG. 3. Photoelectron energy distribution curves of nickel at $h\nu = 10.2$ eV as a function of sample age; (a) $t = 8$ min, (b) $t = 25$ min, (c) $t = 2$ h, and (d) $t = 5$ h after evaporation.

III. RESULTS

A. Near-Normal-Incidence Reflectance Data

The measured reflectance data of Ni at near-normal incidence are presented in Fig. 1, where the number ascribed to a given sample represents the chronological location of a particular "run" in the course of the optical and photoemission studies performed on various elements.

Reflectance measurements have not been made previously in the spectral region above 12 eV, but below this energy, a thorough analysis of existing optical data was made by Ehrenreich *et al.*[5] The data obtained in this work are in very good agreement with their results, particularly for lower photon energies. The samples prepared by Ehrenreich *et al.* were bulk samples, electrolytically etched, whereas the samples used in this work were prepared by vacuum-evaporation techniques.

B. Spectral Distribution of the Quantum Yield

In his review article, Weissler[13] presented data for various metals, showing the pronounced effect of sample treatment on the shape and magnitude of the yield curves. The data of Walker *et al.*[14] for their cleanest samples show that the yield curves reach saturation at roughly 0.02 electrons per incident photon at about 14 eV for Ni and then change very little in magnitude for higher energies up to 26 eV. The photoelectron yield data of Comes and Wenning[15] subtsantiate these results. Cairns and Samson[16] have given the spectral distribution of the yields for samples of Ni prepared by routine polishing and cleaning procedures with no attempt to attain ultrahigh surface purities. Their data are in substantial agreement with the data of Walker *et al.*[14] for untreated samples, the yield curves showing a broad maximum at 17 eV, with a value about four times larger than the yield for clean samples.

The measured photoelectron yield per absorbed photon in our studies is shown in Fig. 2. The magnitude of the yield is in agreement with the values given by Weissler[13] for photon energies of about 12 eV, but at higher energies the yield rises above his saturation value by a factor of about 4. The shape of the spectral distribution curve is not at all like the curves shown in Weissler's review for untreated samples. Curves of the same general shape have been obtained for evaporated films of Pd and Cu.[12]

C. Time-Dependent Energy Distribution Curves

The energy distribution curves for a given incident photon energy measured over a period of 5 h at 3×10^{-8} Torr are shown in Fig. 3. In general, these data reveal surface features that materialize during storage *in vacuo*. The shape of the distribution was not distorted appreciably in the first half-hour after preparation; however, in the subsequent lapse of time, considerable distortion does appear.

When comparing the present energy distribution curves for a freshly prepared surface with previously published data, the time dependence shown in Fig. 3 is significant. The data of Blodgett,[17] Blodgett and

[13] G. L. Weissler, in *Handbuch der Physik*, edited by S. Flügge (Springer-Verlag, Berlin, 1956), Vol. 21, pp. 342–382.
[14] W. C. Walker, N. Wainfan, and G. L. Weissler, J. Appl. Phys. **26**, 1366 (1955).
[15] F. J. Comes and U. Wenning, Phys. Letters **23**, 537 (1966).
[16] R. B. Cairns and J. A. R. Samson, J. Opt. Soc. Am. **56**, 1568 (1966).
[17] A. J. Blodgett, Stanford University Electronics Laboratories Technical Report No. 5205-2, 1965 (unpublished).

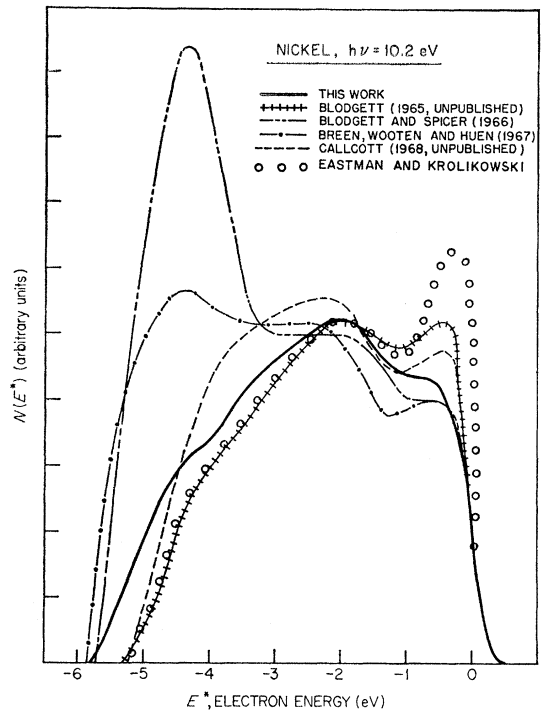

FIG. 4. Comparison of photoelectron energy distribution curves from various authors for nickel at $h\nu = 10.2$ eV.

Spicer,[2] Breen *et al.*,[18] Callcott,[19] and Eastman and Krolikowski[20] are shown together with the results of this work in Fig. 4. The curves are normalized at $E^* = -2.0$ eV to compare the relative intensities of the features in the data. The data reported by Blodgett for "abnormal" Ni show the same general characteristics as the freshly evaporated film data of this work, while Blodgett and Spicer's data for the "normal" form of Ni reveal pronounced structure at $E^* = -5$ eV, suggestive of the surface effects observed for the aged samples.

The recent data of Eastman and Krowlikowski, taken at pressures of $\sim 10^{-10}$ Torr, show general agreement with the results in the present study. In addition, they were able to resolve a much sharper peak at $E^* = -0.2$ eV. X-ray and electron-diffraction studies on their evaporated films indicated polycrystalline fcc Ni with ~ 100- to 150-Å grain size.

D. Frequency-Dependent Energy Distribution Curves

The photoelectron energy distribution curves obtained using photon energies in the spectral range of 10.2–22.4 eV are given (in conjunction with the optical data) in Fig. 5. Each distribution curve represents the average of at least three independent measure-

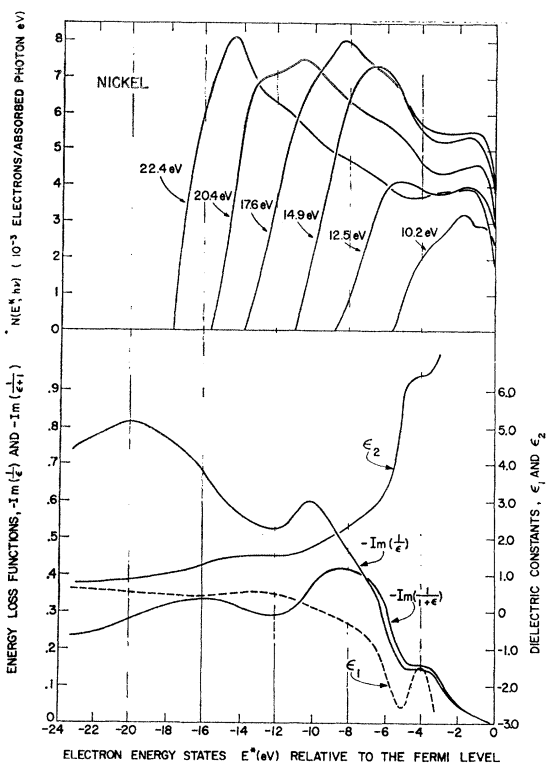

FIG. 5. Photoelectron energy distribution curves and optical constants of nickel in the vacuum uv.

ments using different samples. The relative magnitudes of the structure evident in the data are uncertain by roughly ±15%, but the location of the structure appeared consistently for each sample at an energy $(E^* \pm 0.5)$ eV.

IV. ANALYSIS AND DISCUSSION

A. Optical Properties

The optical properties n and k, the real and imaginary parts of the complex refractive index, were determined by a Kramers-Kronig analysis of the measured near-normal-incident reflectance data up to 24 eV, as described earlier.[21,22] The contribution to the dispersion integral due to the reflectance for photon energies above 24 eV was obtained using values of n and k determined separately for a few selected photon energies in the spectral region of 10.2–22.4 eV. These independent values of n and k were determined using a least-squares fit to Fresnel's equations of the reflectances measured as a function of angle of incidence and the measured polarization[23,24] of the incident flux.

[18] W. M. Breen, F. Wooten, and T. Huen, Phys. Rev. **159**, 475 (1967).
[19] T. A. Callcott (private communication).
[20] D. E. Eastman and W. F. Krolikowski, Phys. Rev. Letters **21**, 623 (1968).
[21] R. A. MacRae, E. T. Arakawa, and M. W. Williams, Phys. Rev. **162**, 615 (1967).
[22] E. T. Arakawa and M. W. Williams, J. Phys. Chem. Solids **29**, 735 (1968).
[23] R. N. Hamm, R. A. MacRae, and E. T. Arakawa, J. Opt. Soc. Am. **55**, 1460 (1965).
[24] V. G. Horton, E. T. Arakawa, R. N. Hamm, and M. W. Williams, Appl. Opt. **8**, 667 (1969).

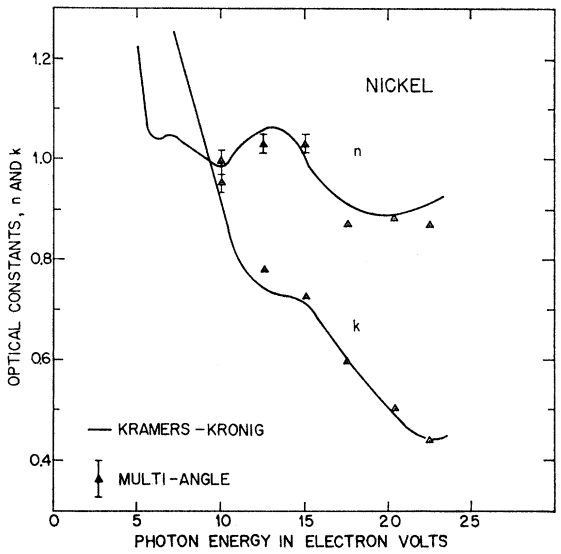

FIG. 6. Values of n and k of nickel as a function of photon energy.

The values of n and k obtained using the multiangle method are shown in Fig. 6 together with those obtained from the Kramers-Kronig analysis.

The real and imaginary parts of the complex dielectric constant $\epsilon=\epsilon_1+i\epsilon_2$, calculated using the optical constants resulting from the Kramers-Kronig analysis, are shown in Fig. 5. The relationships $\epsilon_1=n^2-k^2$ and $\epsilon_2=2nk$ were used in these calculations. Also shown in Fig. 5 are the energy loss functions $-\mathrm{Im}(1/\epsilon)$ and $-\mathrm{Im}(1/\epsilon+1)$, which are related to the probability that a high-energy charged particle will lose energy on traversing the bulk or surface, respectively, of the material.

Although ϵ_1 and ϵ_2 have roughly free-electron-like energy dependences at low photon energies, evidences of single-electron excitation appear throughout the region included in the data. In fact, the optical data in the far infrared (Lenham and Treherne,[25] Dold and Mecke,[26] Shkliarevskii and Padalka,[27] and Beattie and Conn[28]) indicate that the true free-electron properties of the metal do not appear even in the limit of experimental measurements at about 0.6 eV. It is not possible to perform a separation of the free- and bound-electron contributions $\epsilon^{(f)}$ and $\delta\epsilon^{(b)}$ to the dielectric functions, as suggested by Ehrenreich and Philipp,[29] because this separation requires sufficient data in the infrared to establish the free-electron behavior of $\epsilon^{(f)}$ in terms of a constant intraband relaxation time. Thus, the interpretation of the data must necessarily allow for the combined effects of free- and bound-electron behavior.

The effects of single-electron interband transitions are evident in ϵ_1 and ϵ_2 at 4.5 and 14.0 eV in Fig. 5. The strengths of these effects cause the structure to stand out clearly from the free-electron character of the functions. Distinct structure[30] associated with surface plasmon excitation appears at about 8.0 eV and with volume plasmon excitation at 10 and 20 eV in the energy-loss functions.

Robins and Swan[31] summarized the electron energy losses observed experimentally for Ni. Energy losses corresponding to the peak in ϵ_2 at 4.5 eV were observed by several authors (Robins and Swan,[31] Kleinn,[32] Marton and Leder,[33] and Watanabe[34]) in the energy region extending from 4.3 to 6.5 eV. The losses observed by Robins and Swan at 8.3 eV and by Marton and Leder at 9.4 eV can be correlated with peaks in the surface and volume plasma loss functions at 8 and 10 eV, respectively. The lower-energy electrons (1.2 keV) reflected from a solid target by Robins and Swan had a high probability of exciting surface plasmons, whereas the high-energy electrons (20–30 keV) transmitted through thin Ni films by Marton and Leder were more likely to excite volume plasmons. The interband effect at 14.0 eV is evident in the energy-loss measurements of Lang,[35] Marton and Leder, and Watanabe at energies of 15.0, 13.2, and 12.0 eV, respectively. Finally, the energy-loss data of Robins and Swan, Kleinn, Marton and Leder, and Gauthe[36] reveal losses of 19.5, 21.8, 17.6, and 20.6 eV, respectively, to be compared with the maximum in the energy-loss function $-\mathrm{Im}(1/\epsilon)$ at 20.0 eV.

B. Photoemission Properties

The energy distribution curves, using six different photon energies from 10.2 to 22.4 eV, are shown in the upper portion of Fig. 5. The energy distribution curves for higher photon energies are dominated by the large peak at the low-energy end of the distribution curves, and this structure is attributed to the combined effect of inelastic electron-electron scattering within the volume of the metal and at the surface. At the high-energy end of the distribution curves, just below the Fermi level, the structure in the data arises from the high density of states at the top of the d band in Ni. The initial peak lies less than 0.5 eV below the Fermi level, and an additional peak, prominent in the 10.2-eV curve (see also Fig. 3), appears at about 1.6 eV below the Fermi level, but these two pieces of structure are not resolved at higher photon energies. The work

[25] A. P. Lenham and D. M. Treherne, J. Opt. Soc. Am. **56**, 1137 (1966).
[26] B. Dold and R. Mecke, Optik **22**, 454 (1965).
[27] I. N. Shkliarevskii and V. G. Padalka, Opt. i Spektroskopiya **6**, 45 (1959) [English transl.: Opt. Spectry. (USSR) **6**, 45 (1959)].
[28] J. R. Beattie and G. K. T. Conn, Phil. Mag. **46**, 989 (1955).
[29] H. Ehrenreich and H. R. Philipp, Phys. Rev. **128**, 1622 (1962).
[30] H. Ehrenreich and H. R. Philipp, in *Proceedings of the International Conference on the Physics of Semiconductors, Exeter*, (The Institute of Physics and the Physical Society, London, 1962), p. 367.
[31] J. L. Robins and J. B. Swan, Proc. Phys. Soc. (London) **76**, 857 (1960).
[32] W. Kleinn, Optik **11**, 226 (1954).
[33] L. Marton and L. B. Leder, Phys. Rev. **94**, 203 (1954).
[34] H. Watanabe, J. Phys. Soc. Japan **9**, 920 (1954).
[35] W. Lang, Optik **3**, 223 (1948).
[36] B. Gauthé, Ann. Phys. (Paris) **3**, 915 (1958).

function of Ni, as determined from the maximum energy of the photoelectrons, was found to be in good agreement with the estimate of 4.5 eV by Fomenko.[3] Finally, structure persists in the energy distribution curves at E^* equal to -5.0 and -10.5 eV for changing photon energies.

The structure at 0.5 and 1.6 eV below the Fermi level in the energy distribution curves, shown most clearly in Fig. 3, is identified with shoulders reported in ϵ_2 by Beattie and Conn,[28] Roberts,[37] and Ehrenreich *et al.*[5] at 0.3 and 1.4 eV. Ehrenreich *et al.* associate both shoulders with interband effects involving transitions between the d band and the Fermi surface.

Blodgett and Spicer[2] associate the structure at $E^*=-5.0$ with anomalous structure appearing in the density of electronic states of Ni. This observed structure was deemed "anomalous" because it does not appear in the density of states of Ni calculated by use of the rigid-band model and the Cu density of states. The results of soft x-ray emission measurements by Cuthill *et al.*[38] and the ion-neutralization studies of Hagstrum[39] confirm the existence of structure in the density of electronic states at 4.5 eV below the Fermi level, but the data are in disagreement with Blodgett and Spicer's results concerning the magnitude of the peak. The theoretical band-structure calculations of Connolly[40] and Snow *et al.*[41] favor a low intensity peak at $E^*=-4.5$ eV. The photoemission studies presented here include data with sufficient excitation energies to enable measurement of emitted electrons with $E^*=-5$ eV well separated from the electron-electron scattering peak at the low-energy end of the distribution. This structure persists with changing photon energy, and may be attributed to strength in the optical-transition-probability function for 5-eV transitions or to a discrete energy-loss process of about 4.5 eV suffered by the electrons excited from the d band, which peaks roughly 0.5 eV below the Fermi level.[4,42] Support is given to the latter possibility by the pronounced structure evident in ϵ_2 at 4.5 eV and by the discrete characteristic energy loss observed by Robins and Swan[31] in the region of 4.3 eV.

The structure at $E^*=-10.5$ eV can be associated with the structure in the energy-loss function $-\mathrm{Im}(1/\epsilon)$ at about the same energy. Since ϵ_2 is without pronounced structure in this region, the structure in the energy distribution curves may be attributed to a discrete energy loss of about 10 eV suffered by the photoelectrons in excitation of volume plasmons. An energy loss in the photoemission data of about 10 eV compares favorably with the loss reported by Marton and Leder of 9.4 eV, obtained for high-energy electrons. The data presented in this paper support the conclusion that low-energy photoelectrons, excited within the metal, may lose discrete amounts of energy in the same way as electrons with many times more energy. Furthermore, it appears from these data that the optical-energy-loss functions, derived originally with the assumption that the momentum vector of the incident electron changes only by a negligible amount on scattering, may be valid even under the quite different conditions present in the photoemission process.

V. SUMMARY

Studies of the time-dependent changes in the photoelectron energy distribution curves at 10.2 eV revealed the pronounced effect of contaminants on the surface of the freshly prepared sample even under ultrahigh vacuum conditions. The changes were characterized by the development of a strong peak in the energy distribution curves at low electron energies. The appearance of such structure was very sensitive to the surface properties of the sample and was used as a measure of its surface quality.

Structure in the energy distribution curves determined for selected excitation energies in the region of 10.2 to 22.4 eV has been interpreted in terms of the measured optical data. Very good correlations were possible for the structure in the energy distribution curves within about 5 eV of the Fermi level, and the origins of the structure were correlated with relative peaks in the density of electronic states in the valence band that account for the large excitation probabilities. The same reason was given for the appearance of the related structure in the imaginary part of the complex dielectric function.

Structure in the energy distribution curves lying well below the Fermi level was more difficult to identify unambiguously.

Some persistent structure in the energy distribution curves was evident, and interpretation of these results as energy-loss processes was shown to be consistent with the optical data and the independent characteristic energy-loss measurements. These results support the contention that discrete energy losses play a significant role in the determination of the density of electronic states using photoemission data. Also, the results suggest that even near the thresholds for inelastic scattering of electrons, a valid interpretation of the data was possible on the basis of the optical properties of the sample.

ACKNOWLEDGMENTS

The authors wish to acknowledge helpful discussions with Dr. R. H. Ritchie and Dr. M. W. Williams on some theoretical aspects of this work. We also thank Dr. T. A. Callcott for sending us a report of his work.

[37] S. Roberts, Phys. Rev. **114**, 104 (1959).
[38] J. R. Cuthill, A. J. McAlister, M. L. Williams, and R. E. Watson, Phys. Rev. **164**, 1006 (1967).
[39] H. D. Hagstrum, Phys. Rev. **150**, 495 (1966).
[40] J. W. D. Connolly, Phys. Rev. **159**, 415 (1967).
[41] E. C. Snow, T. J. Waber, and A. C. Switendick, J. Appl. Phys. **37**, 1342 (1966).
[42] R. K. Nesbet and P. M. Grant, Phys. Rev. Letters **19**, 222 (1967).